Investigation the structural and surface characteristics of irradiated flexible polymeric nanocomposites films

A. W. Alrowaily [a], B. M. Alotaibi [a], A. Atta [b,*], E. Abdeltwab [b], M. M. Abdelhamied [c]

[a] *Department of Physics, College of Science, Princess Nourah bint Abdulrahman University, P.O. Box 84428, Riyadh 11671, Saudi Arabia*

[b] *Physics Department, College of Science, Jouf University, P.O. Box: 2014, Sakaka, Saudi Arabia*

[c] *Radiation Physics Department, National Center for Radiation Research and Technology (NCRRT), Egyptian Atomic Energy Authority (EAEA), Cairo, Egypt*

This study is to investigate the surface and structural characteristics of the pure and irradiated novel PEO/NiO composite by subjecting the films to argon ions with different ion beam fluencies. The structural characteristics were studied by the EDX and FTIR techniques, while the surface was investigated by SEM technique. The FTIR showed a notable decrease in the peak intensity for the bombarded composite, due to the functional groups with hydrophilic characteristics and the occurrence of chain scission processes. The PEO/NiO composite demonstrates a consistent structure without any nanoparticle clusters, as depicted in the SEM image of PEO/NiO. Moreover, the electrical conductivity for the pure and the irradiated samples were determined. Exposing the composite PEO/NiO to a fluence of 15×10^{16} ions.cm^{-2}, increasing the conductivity from 7.5×10^{-8} S/cm to 8.4×10^{-7} S/cm. By increasing ion fluence from 5×10^{16} to 15×10^{16} ions.cm^{-2}. The contact angle is decreased from 81.15° to 72.22° for water, while is decreased from 74.32° to 62.20° for diiodomethane. Moreover, the surface wettability and the adhesion force were determined from the data of the contact angle. The work of adhesion of water increases from 84.37 to 94.16 mJ/m^2 and for dioodomethane from 64.52 to 74.49 mJ/m^2, respectively, by increasing ion fluence from 5×10^{16} to 15×10^{16} ions.cm^{-2}. This suggests that, in comparison to a unirradiated surface, the increase in W_a is the result of surface cleanliness following radiationThe results of this study show the opportunities for utilizing these irradiated materials in the fields of coating and printing applications.

(Received August 11, 2024; Accepted October 29, 2024)

Keywords: Nanocomposite, Ionization, Surface modifications, Electrical conductivity

1. Introduction

The polymer nanocomposites are combined novel properties of nanofillers properties and polymers characteristics, leading to advancements in electronics, coatings, sensors, and other diverse domains [1, 2]. The current research in this field has the potential to reveal further customized and advanced uses for polymer nanocomposites in several industries [3, 4]. The higher electrical conductivity leads to improved charge/discharge rates and overall performance [5, 6]. In addition, polymer nanocomposites are employed in actuators designed for constructions that are responsive and adaptive, that are widely used in the fields of electronics, telecommunications, and aerospace [7].

Polyethylene oxide (PEO) exhibits numerous fundamental characteristics [8]. PEO is a category of materials that possess distinctive qualities, capabilities, and applications in diverse industries [9, 10]. PEO exhibits biocompatibility, rendering it appropriate for utilization in biomedical applications, including controlled drug release systems, tissue engineering, and medical devices. This characteristic is beneficial in the advancement of polymer electrolytes and medication delivery systems [11]. Polymer electrolytes based on polyethylene oxide (PEO) are utilized in

* Corresponding author: aam86718@gmail.com
https://doi.org/10.15251/DJNB.2024.194.1655

lithium-ion batteries and other electrochemical devices to significantly improve ionic conductivity and overall performance [12].

Nickel oxide (NiO) is a type of oxide displays unique characteristics in terms of its electrical and optical properties. NiO is usefulness in many electronic devices, including transistors, sensors, and solar cells. NiO exhibits intriguing optical characteristics, such as its capacity to absorb and emit light within the visible spectrum [13]. This feature enables its use in optoelectronic devices and smart windows. NiO is renowned for its catalytic prowess, especially in oxidation-reduction reactions. It is utilized as a catalyst in chemical reactions and as an electrode material in electrochemical cells. NiO serves as a catalyst in several chemical reactions, such as oxidation processes utilized in chemical manufacturing and environmental cleanup [14]. NiO's semiconductor characteristics render it well-suited for utilization in solar cells and other photovoltaic devices [15].

Extensive research has been conducted to improve the structural and functional qualities of composites via ion beam [16]. An innovative technique that has garnered attention is the utilization of ion irradiation. The ion beams can be used to deliberately modify polymers at both the molecular and surface levels, resulting in composite materials with distinct properties [17]. This novel method provides a means to customize the characteristics of polymer composites for particular uses, encompassing enhancements in mechanical strength, thermal stability, adhesion, and wettability [18]. Ion beam irradiation at low energy levels causes the formation of chemical bonds between polymer chains, resulting in enhanced mechanical strength and dimensional stability [19]. On the other hand, chain scission can happen, which changes the size of the polymer molecules and affects characteristics such as flexibility and viscosity [20].

The distinctive feature of this study Is In the utilization of a low-energy source as friendly technique to stimulate the surface characteristics of the produced films. In addition, this low-energy ion source operates without generating heat. In this study the EDX, FTIR and SEM were used to analyze the structural and morphological of the irradiated films. Furthermore, the electrical characteristics will be conducted. The results indicated that the irradiated PEO/NiO showed enhancements in its structure, wettability and electrical conductivity to apply in various electronic devices.

2. Experimental work

The polyethylene oxide powder (PEO) with a molecular weight of 99,800 was obtained from Sigma Aldrich Company. The nickel (II) oxide nanoparticles with a size of 45 nm (99.7% purity) were acquired also from the same company. The PEO/NiO film was made using the solution casting process, as previously described [21, 22], by adding 0.6 gm of the PEO and rapidly stirring for 6 hours at a temperature of 60 ^{o}C. Next, 0.03 g of the nickel oxide (NiO) nanopowder was dissolved in 8 ml of tetrahydrofuran (THF), and the mixture was subjected to sonication and stirring for a duration of 4 hours. Ultimately, the combined mixture is exposed to the air for a duration of 3 days to allow for drying. Each film was divided into 1cm x 1cm. Then the films were bombarded using varying fluences of the Ar ion (5×10^{16}, 10×10^{16}, and 15×10^{16} ions.cm^{-2}). The ion source, as depicted in Figure 1, consists of extraction electrodes and ionization medium, as described in a prior study [23]. The ion source operating conditions are pressure of 2.3×10^{-4} mbar and an energy of 4 keV.

The FTIR absorbance (Shimadzu FTIR-340) was used to analyze the pure and treated samples by FT-IR. The composition of the composite is determined through investigation utilizing (EDX, JEOL, Japan). The conductivity is determined using an LCR meter in frequency of 50 Hz to 1 MHz. The contact angles were determined to estimate the work of adhesion and the surface free energies.

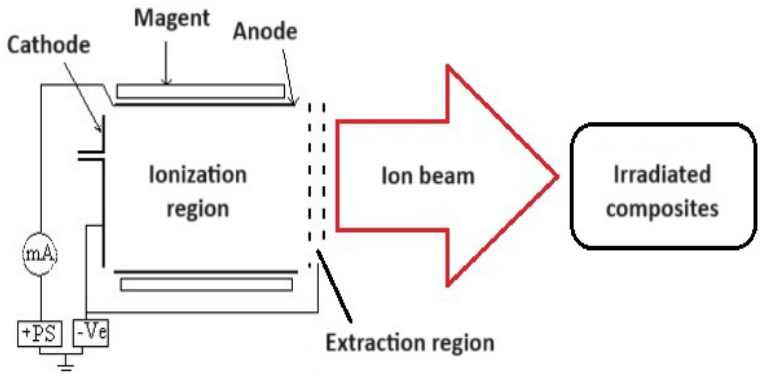

Fig. 1. Schematic figure of broad beam source.

3. Results and discussion

Figure 2a investigate the SRIM/TRIM simulations [24] of 4 keV argon bombarded with PEO/NiO films at a depth range of 21.7 nm. When ion beam collided the atoms, enough energy is released to allow the recoiled atoms to separate from the network and interact with one other. It is shown in Figure 2b, the ions are much less affected by the argon beam for phonons than the recoiled atoms. Figure 2c also shows the cases of argon ion collisions with target vacancies that damaged the target.

Figure 3a displays the chemical composition of the PEO/NiO composite using EDX spectra. By analyzing the distinct peaks in the EDX spectrum, the composition of carbon, argon, and nickel is respectively determined as 60%, 38%, and 2%. The generated composite did not contain any additional impurities. The PEO/NiO composite demonstrates a consistent structure without any nanoparticle clusters, as depicted in the scanning electron microscopy (SEM) image of PEO/NiO in Figure 3b. The EDX study provides of a significant integration between PEO and NiO [25].

The FTIR analysis were measured for pure and irradiated films as shown in Figure 4. It can be observed that the absorbance of the PEO/NiO film displays the typical peaks of the PEO and NiO. In which, the absorbance peaks at 2869.81, 1461.9 cm^{-1} are ascribed to the C–H group and CH_2 scissoring in PEO polymer, respectively [26]. Moreover, the wagging CH_2 and C-O-C mode of PEO matrix was also revealed at 1340 and 1145.3 cm^{-1}, respectively [27]. The CH_2 symmetric twisting of the PEO was also appeared at wavenumber 1276.75 and 1238.18 cm^{-1} [28]. The two bands adjacent ones at 950.81 and 838.95 cm^{-1} recorded the rocking CH_2 bonds of the PEO. In this spectrum, appearing large peak at 1093.5 cm^{-1} is for C–O–C triple band which confirms that the PEO was formed in the nanocomposite film as semicrystalline phase [29]. In addition to that, this spectrum also shows a broad band with low intensity at 3452.25 cm^{-1} which is explained to the OH vibrations of both PEO and NiO.

The other peaks of the NiO were also given at 2229 and 1639.41 cm^{-1} for the stretching C = C of alkyne molecules and the OH group [30]. The spectrum of the irradiated spectra by different fluence of Ar ion beam show that the spectra are seeming repetitive with minor variations in the position, breadth and intensity of bands. For example, the peak at 950.81 cm^{-1} was shifted to 951.71 and 952.34 cm^{-1} after irradiation by $10x10^{16}$ and $15x10^{16}$, respectively. Further, peaks at 1093.5, 1238.1, 1276.8, 1346.2, 2869.8, 3452.3 cm^{-1} were also shifted after the ion irradiation. Meanwhile, the intensity of peaks at 950.8, 1093.5 and 1461.9 cm^{-1} were decreased and broaden after irradiation, which are due to the reduction in the semicrystalline nature of polymer. These changes in intensity and position peaks upon irradiation confirm changes of the nanocomposite [31]. These results record that the disorder in the irradiated films and thus the amorphous content was increased, which support improving the electrical properties of the irradiate films.

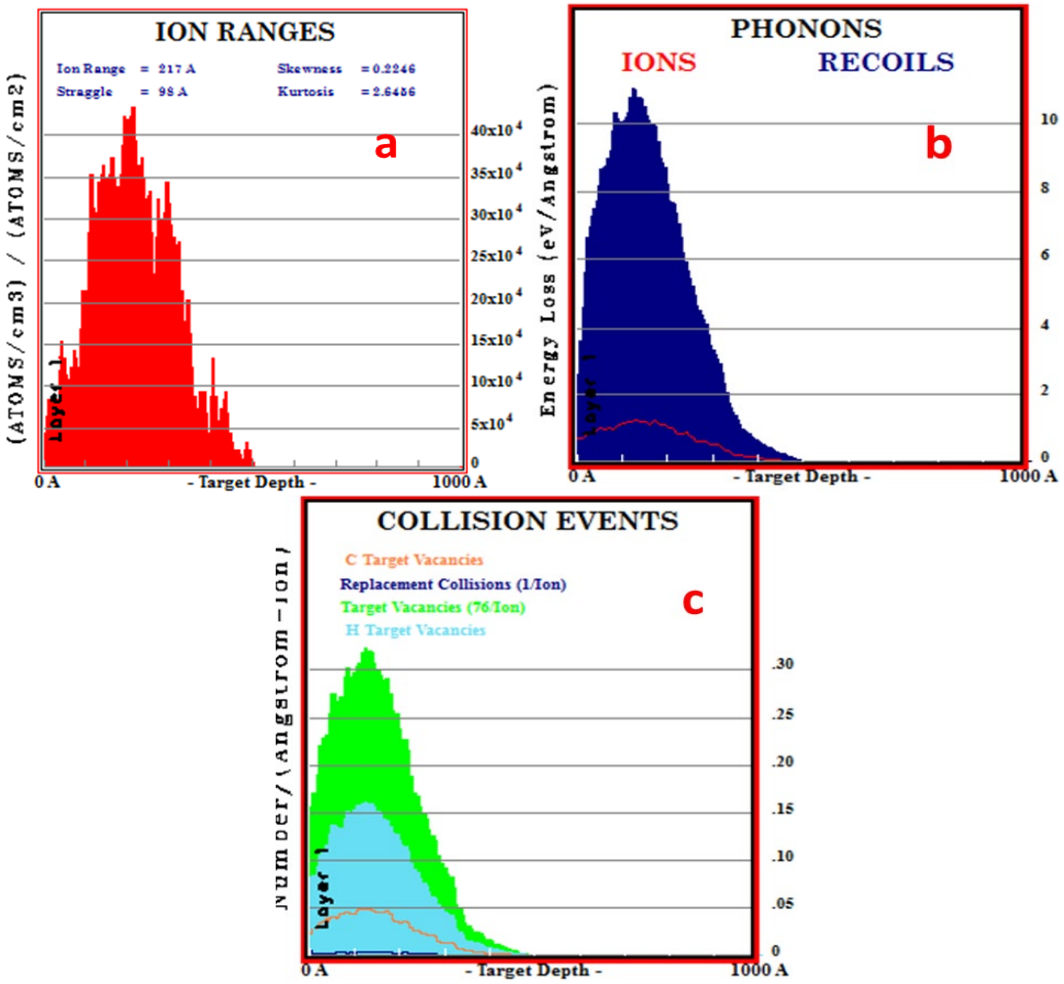

Fig. 2. a) Argon ions depth with PEO/NiO, b) the Phonos of the recoils atoms and implanted argon ions in PEO/NiO, c) distribution of Ar with PEO.

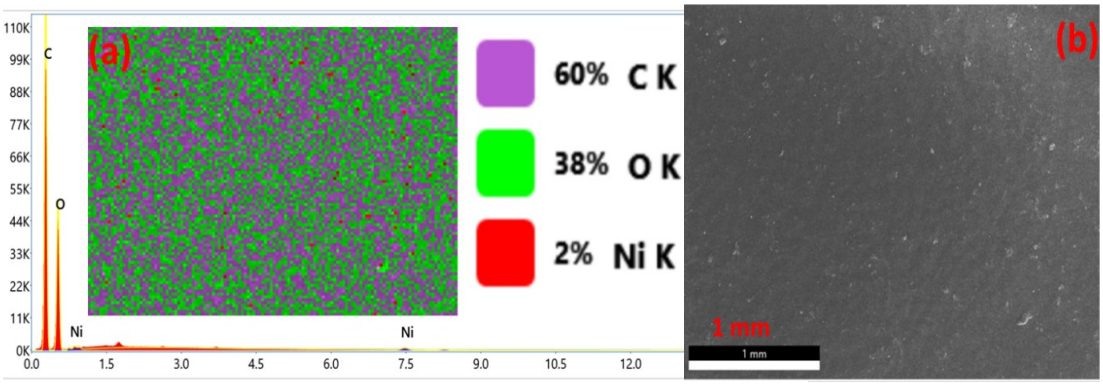

Fig. 3. (a) EDX spectra and (b) SEM image, of the fabricated of PEO/NiO composite.

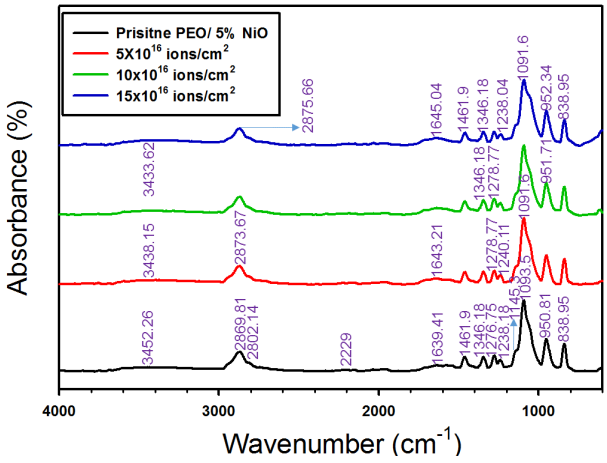

Fig. 4. FTIR of the pure and treated composites.

The contact angle of untreated and irradiated PEO/NiO with different fluencies is illustrated in Figure 5. Table 1 illustrate the angle reduces as the ion bombardment increases. The creation of functional groups for the irradiated samples, leading to a reduction in the angle value [32]. By enhancing fluence from 5×10^{16} to 15×10^{16} ions/cm^2, the angle of water is decreased from 81.15° to 72.22°, while is decreased from 74.32° to 62.20° for diiodomethane. This reduction is achieved by increasing the irradiation fluence from 5×10^{16} ions/cm^2 to 15×10^{16} ions/cm^2, as indicated in Table 1. The angle of all treated samples is reduced compared to pure films, suggesting that the properties become more hydrophilic after irradiation.

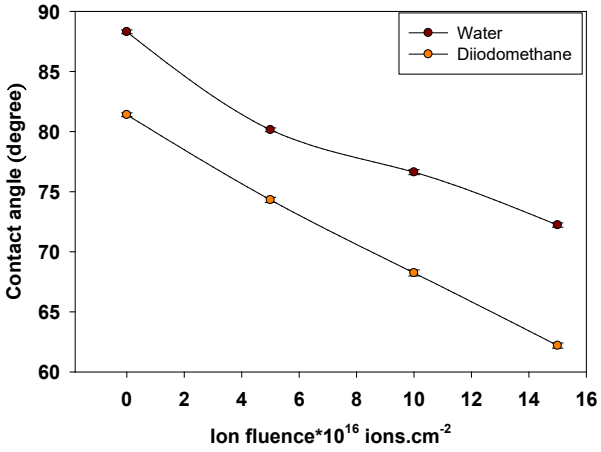

Fig. 5. The contact angle of pure and treated PEO/NiO films.

The next equation is to estimate the adhesion work W_a, which corresponds to the energies of interaction between molecules across the interface, using surface energy liquid (γ_l) and the angle (θ) [33].

$$W_a = \gamma_l(1 + cos\theta) \quad (1)$$

Fig. 6 illustrates the work of adhesion W_a as a consequence of argon beam. Table 1 show that the W_a for water liquids increases from 84.37 to 94.16 mJ/m^2 and for dioodomethane from 64.52 to 74.49 mJ/m^2, respectively, when irradiation goes up from 5×10^{16} ions/cm^2 to 15×10^{16} ions/cm^2.

This suggests that, in comparison to a unirradiated surface, the increase in W_a is the result of surface cleanliness following radiation[34].

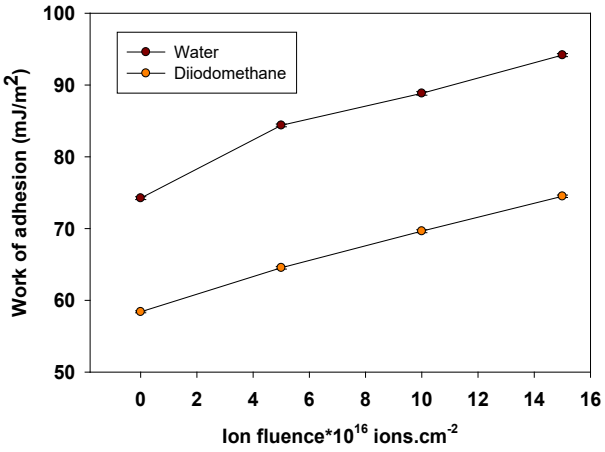

Fig. 6. The W_a of pure and irradiated PEO/NiO films.

Table 1. The θ and W_a for pristine and irradiated PEO/NiO.

	Contact angle		Work of adhesion	
	Water	Diiodomethane	Water	Diiodomethane
PEO/NiO	88.30	81.40	74.23	58.39
5×10^{16} ions/cm^2	80.15	74.32	84.37	64.52
10×10^{16} ions/cm^2	76.62	68.24	88.83	69.63
15×10^{16} ions/cm^2	72.22	62.20	94.16	74.49

The surface energy of PEO/NiO is calculated by [35].

$$\frac{\gamma_l(1+\cos\theta)}{2\sqrt{\gamma_l^d}} = \sqrt{\gamma_s^d} + \sqrt{\gamma_s^p}\cdot\sqrt{\frac{\gamma_l^p}{\gamma_l^d}} \tag{2}$$

where, the interfacial parameters is γ_s for solid vapor, γ_{sl} for solid-liquid, and γ_l for liquid-vapor. The surface free energy of pure and irradiated PEO/NiO is displayed in Figure 7. Table 2 shows that free energy (γ_s^t) increases from 29.76 to 38.14 mJ/m^2 by raising the radiation from 5×10^{16} to 15×10^{16} ions/cm^2. The polar surface energy (γ_s^p) increases from 9.27 to 10.83 mJ/m^2, while (γ_s^d) increases from 20.49 to 38.14 mJ/m^2. The polar and/or hydrophilic forming groups are responsible for the improvement in the polar and dispersive surface energy [36].

Table 2. The γ_s^p, γ_s^d, and γ_s^t for pure and treated PEO/NiO.

	Polar γ_s^p (mJ/m^2)	Dispersive γ_s^d(mJ/m^2)	total γ_s^t (mJ/m^2)
PEO/NiO	6.80	16.78	23.59
5×10^{16} ions/cm^2	9.27	20.49	29.76
10×10^{16} ions/cm^2	9.81	23.86	33.67
15×10^{16} ions/cm^2	10.83	27.30	38.14

As a result, compared to the un-irradiated films, the irradiated films have greater hydrophilicity and wettability [37]. These findings demonstrate that the PEO/NiO surface wettability is improved for the treated PEO/NiO due to the enhanced of polarity by irradiation. The changes of morphology, polarity, and structural induced by ion beam treatments are responsible for this enhancement in the surface wettability of the irradiated samples [38].

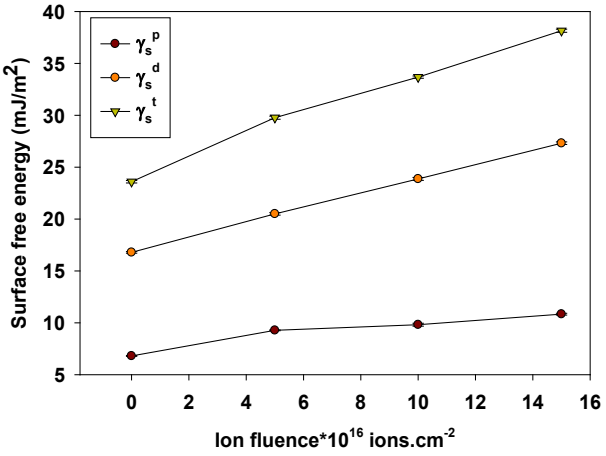

Fig. 7. Polar, dispersive and total surface energy for pristine and treated PEO/NiO samples.

The σ_{ac} conductivity is given by [39].

$$\sigma_{ac} = 2\pi f \varepsilon_o \varepsilon'' \tag{3}$$

The frequency-dependent variation of σ_{ac} for pure and treated PEO/NiO is plotted in figure 8. By increasing the frequency, the conductivity σ_{ac} is noticeably increases [40]. For the un-irradiated PEO/NiO film, electrical conductivity at frequency 50 Hz rose from $7.5\text{x}10^{-8}$ to $2.1\text{x}10^{-7}$, $2.9\text{x}10^{-7}$ and $8.4\text{x}10^{-7}$ S/cm after irradiation respectively with $5\text{x}10^{16}$, $10\text{x}10^{16}$ and $15\text{x}10^{16}$ ions/cm^2. An rise in conductivity as a consequence of radiation is most likely caused by developments in the ability to move of the carriers of charges, which are in charged hopping and electronic polarization [41].

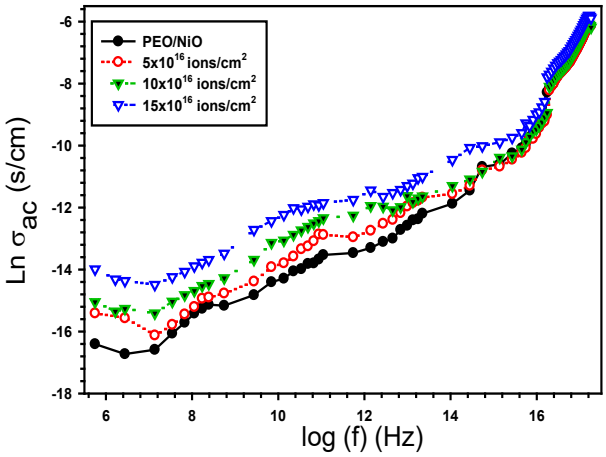

Fig. 8. The σ_{ac} of the pure and irradiated PEO/NiO.

On the other hand, at shorter frequencies, this relationship describes the fluctuation in dielectric loss is given by[42].

$$\varepsilon'' = A\omega^m \tag{4}$$

The plots of ln (ε'') with ln ω is shown in Figure 9. The power m value is given from the slopes of these lines as in figure 9. Moreover, the height barrier energy (W_M) needed to move were calculated by [43].

$$W_m = \frac{-4k_BT}{m} \tag{5}$$

The average value of W_m declined from 4.9 eV pure sample to 3.5, 3.2, and 2.2 eV for $5x10^{16}$, $10x10^{16}$, and $15x10^{16}$ ions.cm^{-2}, respectively. This fall in W_m values can be attributed to the formation of flaws in the bombarded films. The polarization changed by these defects, which are the result of homopolar connections of the bands of valence and conduction [43].

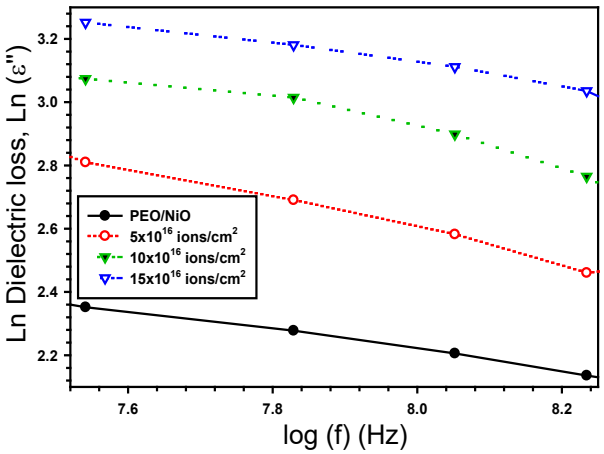

Fig. 9. Ln ε'' with frequency for pristine and irradiated PEO/NiO.

4. Conclusions

In this study, the PEO/NiO samples were synthesize by the solution casting method. The PEO/NiO samples were characterized by using FTIR, SEM, and EDX techniques. The techniques proved the successful preparations of the composites. Then the ion source was used to radiate the flexible PEO/NiO sheets with differ ion fluencies. Then the contact angle was determined for all samples, which shows, it is less for all bombarded sheets than for un-irradiated films. The adhesion work and surface energy have been computed from the data of the contact angle. The surface energy increases from 29.76 to 38.14 mJ/m^2 by raising the radiation from 5×10^{16} to 15×10^{16} ions/cm^2. The polar energy increases from 9.27 to 10.83 mJ/m^2, while the dispersive increases from 20.49 to 38.14 mJ/m^2. Moreover, the electrical conductivity for PEO/NiO in the frequency range of 50 Hz to 5 MHz were recorded. The results demonstrate that the exposure to ion beam irradiation modified the surface morphology, chemical structure, electrical conductivity, and surface wettability of the bombarded films to be more convenient in energy applications.

Acknowledgements

Princess Nourah bint Abdulrahman University Researchers Supporting Project number (PNURSP2024R378), Princess Nourah bint Abdulrahman University, Riyadh, Saudi Arabia.

References

[1] Abdelhamied, M. M., Gao, Y., Li, X., Liu, W. (2022), Applied Physics A, 128(1), 57; https://doi.org/10.1007/s00339-021-05189-y

[2] Hassan, H. B., Abduljalil, H. M., Hashim, A. (2021), Physics and Chemistry of Solid State, 22(3), 501-508; https://doi.org/10.15330/pcss.22.3.501-508

[3] Abdeltwab, E., Atta, A., Bek, A. L. P. A. N. (2022), International Journal of Modern Physics B, 36(20), 2250125; https://doi.org/10.1142/S0217979222501259

[4] Khdary, N. H., Almuarqab, B. T., El Enany, G. (2023), Membranes, 13(5), 537; https://doi.org/10.3390/membranes13050537

[5] Atta, A., Abdeltwab, E., Negm, H., Al-Harbi, N., Rabia, M., Abdelhamied, M. M. (2023), Journal of Inorganic and Organometallic Polymers and Materials, 1-13; https://doi.org/10.1007/s10904-023-02643-7

[6] Atta, A., Abdeltwab, E., Negm, H., Alshammari, A. H., Abdelhamied, M. M., Ahmed, A. M., Rabia, M. (2023), Physica Scripta, 98(9), 095916; https://doi.org/10.1088/1402-4896/acec18

[7] Al-Bermany, E., Mekhalif, A. T. M., Banimuslem, H. A., Abdali, K., Sabri, M. M. (2023), Silicon, 1-13; https://doi.org/10.1007/s12633-023-02332-7

[8] Mahdi, S. M., Habeeb, M. A. (2023), Polymer Bulletin, 1-20; https://doi.org/10.1007/s00289-023-04676-x

[9] Migdadi, A. B., Ahmad, A. A., Alsaad, A. M., Al-Bataineh, Q. M., Telfah, A. (2023), Polymer Bulletin, 80(5), 5433-5446; https://doi.org/10.1007/s00289-022-04329-5

[10] Althubiti, N. A., Atta, A., Al-Harbi, N., Sendi, R. K., Abdelhamied, M. M. (2023), Optical and Quantum Electronics, 55(4), 348; https://doi.org/10.1007/s11082-023-04600-7

[11] Elashmawi, I. S., Ismail, A. M. (2023), Polymer Bulletin, 80(3), 2329-2348; https://doi.org/10.1007/s00289-022-04139-9

[12] Atta, A., Abdeltwab, E., Negm, H., Al-Harbi, N., Rabia, M., Abdelhamied, M. M. (2023), Inorganic Chemistry Communications, 152, 110726; https://doi.org/10.1016/j.inoche.2023.110726

[13] Asghari, E., Malekian, S. (2017), Synthetic Metals, 229, 57-64; https://doi.org/10.1016/j.synthmet.2017.05.009

[14] Atta, A., Negm, H., Abdeltwab, E., Rabia, M., & Abdelhamied, M. M. (2023), Polymers for Advanced Technologies; https://doi.org/10.1002/pat.5997

[15] Ahmed, S. S., Amiri, O., Rahman, K. M., Ismael, S. J., Rasul, N. S., Mohammad, D., Abdulrahman, N. A. (2023), Scientific Reports, 13(1), 7574; https://doi.org/10.1038/s41598-023-34329-y

[16] Al-Yousef, H. A., Atta, M. R., Abdeltwab, E., Atta, A., Abdel-Hamid, M. M. (2023). Emerging Materials Research, 40, 1-13; https://doi.org/10.1680/jemmr.22.00199

[17] Atta, A., Al-Harbi, N., Alotaibi, B. M., Uosif, M. A. M., Abdeltwab, E. (2024), Inorganic Chemistry Communications, 159, 111651; https://doi.org/10.1016/j.inoche.2023.111651

[18] Althubiti, N. A., Al-Harbi, N., Sendi, R. K., Atta, A., Henaish, A. M. (2023), Inorganics, 11(2), 74; https://doi.org/10.3390/inorganics11020074

[19] Abdeltwab, E., Atta, A. (2022), ECS Journal of Solid State Science and Technology, 11(4), 043012; https://doi.org/10.1149/2162-8777/ac66fe

[20] Althubiti, N. A., Atta, A., Alotaibi, B. M., Abdelhamied, M. M. (2022), Surface Innovations, 11(1-3), 90-100; https://doi.org/10.1680/jsuin.22.00010

[21] Althubiti, N. A., Atta, A., Al-Harbi, N., Sendi, R. K., Abdelhamied, M. M. (2023), Optical and Quantum Electronics, 55(4), 348; https://doi.org/10.1007/s11082-023-04600-7

[22] Alotaibi, B. M., Atta, A., Atta, M. R., Abdeltwab, E., Abdel-Hamid, M. M. (2023), Surface Innovations, 40, 1-12; https://doi.org/10.1680/jsuin.22.01078

[23] Al-Yousef, H. A., Atta, A., Abdeltwab, E., Atta, M. R., Abdel-Hamid, M. M. (2023), International Journal of Modern Physics B, 2450164; https://doi.org/10.1142/S0217979224501649

[24] Hofsäss, H., Zhang, K., Mutzke, A. (2014), Applied Surface Science, 310, 134-141; https://doi.org/10.1016/j.apsusc.2014.03.152

[25] Liang, J., Hwang, S., Li, S., Luo, J., Sun, Y., Zhao, Y., Sun, X. (2020), Nano Energy, 78, 105107; https://doi.org/10.1016/j.nanoen.2020.105107

[26] Abdelghany, A. M., Farea, M. O., Oraby, A. H. (2021), Journal of Materials Science: Materials in Electronics, 32, 6538-6549; https://doi.org/10.1007/s10854-021-05371-1

[27] Telfah, A., Al-Bataineh, Q. M., Tolstik, E., Ahmad, A. A., Alsaad, A. M., Ababneh, R., Hergenröder, R. (2023), Polymer Bulletin, 80(9), 9611-9625; https://doi.org/10.1007/s00289-022-04508-4

[28] Noor, S. A. M., Ahmad, A., Talib, I. A., Rahman, M. Y. (2010), Ionics, 16, 161-170; https://doi.org/10.1007/s11581-009-0385-6

[29] Hassan, H. B., Abduljalil, H. M., Hashim, A. (2021), Physics and Chemistry of Solid State, 22(3), 501-508; https://doi.org/10.15330/pcss.22.3.501-508

[30] Alam, M. W., Baqais, A., Mir, T. A., Nahvi, I., Zaidi, N., Yasin, A. (2023), Scientific reports, 13(1), 1328; https://doi.org/10.1038/s41598-023-28356-y

[31] Raghu, S., Archana, K., Sharanappa, C., Ganesh, S., & Devendrappa, H. (2016), Journal of Radiation Research and Applied Sciences, 9(2), 117-124; https://doi.org/10.1016/j.jrras.2015.10.007

[32] Kallweit, C., Bremer, M., Smazna, D., Karrock, T., Adelung, R., Gerken, M. (2017), Vacuum, 146, 386-395; https://doi.org/10.1016/j.vacuum.2017.03.023

[33] Papakonstantinou, D., Amanatides, E., Mataras, D., Ioannidis, V., Nikolopoulos, P. (2007), Beam Processes and Polymers, 4(S1), S1057-S1062; https://doi.org/10.1002/ppap.200732405

[34] Patra, N., Hladik, J., Pavlatová, M., Militký, J., Martinová, L. (2013), Polymer degradation and stability, 98(8), 1489-1494; https://doi.org/10.1016/j.polymdegradstab.2013.04.014

[35] Young, T. (1805), Philosophical transactions of the royal society of London, (95), 65-87; https://doi.org/10.1098/rstl.1805.0005

[36] Atta, A. (2013), Arab J. Nucl. Sci. Appl, 46(5), 115-123.

[37] Mazaltarim, A. J., Taylor, J. M., Konda, A., Stoller, M. A., Morin, S. A. (2019), ACS applied materials & interfaces, 11(36), 33452-33457; https://doi.org/10.1021/acsami.9b10454

[38] Jaleh, B., Etivand, E. S., Mohazzab, B. F., Nasrollahzadeh, M., Varma, R. S. (2019), International journal of molecular sciences, 20(13), 3309; https://doi.org/10.3390/ijms20133309

[39] Atta, A., Alotaibi, B. M., Abdelhamied, M. M. (2022), Inorganic Chemistry Communications, 141, 109502; https://doi.org/10.1016/j.inoche.2022.109502

[40] Pervaiz S, Kanwal N, Hussain SA, Saleem M, Khan IA (2021), Journal of Polymer Research 28(8): 1-13; https://doi.org/10.1007/s10965-021-02640-9

[41] Abdelhamied, M. M., Abdelreheem, A. M., Atta, A. (2021), Plastics, Rubber and Composites, 1-1; https://doi.org/10.1080/14658011.2021.1928998

[42] A. Hashim, A. Hadi, Ukrainian Journal of Physics 63 (2018) 754-754; https://doi.org/10.15407/ujpe63.8.754

[43] Atta, A., Abdelhamied, M. M., Abdelreheem, A. M., Althubiti, N. A. (2022), Inorganic Chemistry Communications, 135, 109085; https://doi.org/10.1016/j.inoche.2021.109085